Journal of Corrosion and Materials
www.corromat.com

J. Corros. Mater. **49**(1), 2024 1–8
https://doi.org/10.61336/jcm2024-1

Inhibition Study and Adsorption Responses of Copper in Chicken Bone Ash Inhibited NaCl Environment

Ojo S. I. Fayomi[1,2], Joshua O. Atiba[1,*]

[1] *Department of Mechanical Engineering, Bells University of Technology, P.M.B. 1015, Ota, Ogun State, Nigeria*
[2] Department of Mechanical Engineering Science, University of Johannesburg, Auckland Park, Kingsway Campus, Johannesburg, South Africa
(Received: 07 March 2023. Received in revised form: 20 August 2023. Accepted: 01 January 2024. Published online: 30 June 2024.)

Abstract

By examining the corrosive behaviour and adsorption characteristics of copper in a corrosive medium containing 0.5 M NaCl, the potential of chicken bone as a corrosion inhibitor was examined in this study. With inhibitor concentrations ranging from 0.2 to 0.8 g, the experiments were carried out at temperatures between 30 and 60 °C. The effectiveness of chicken bone ash as a corrosion inhibitor was evaluated using a variety of electrochemical analysis techniques, such as polarisation analysis and open circuit potential measurement. The electrochemical analysis' findings demonstrated that chicken bone ash functions as a cathodic inhibitor, significantly slowing copper corrosion. The inhibitor outperformed all other concentrations tested and demonstrated its maximum inhibition efficiency at a temperature of 50°C. These findings were further supported by the adsorption parameter analysis, which showed that the copper surface responded quickly to the inhibitor's adsorption, primarily through a physical adsorption process. A promising alternative for protecting copper in corrosive environments is the use of chicken bone as a corrosion inhibitor. The findings imply that chicken bone ash has inherent inhibitory properties that effectively slow down corrosion.

Keywords: Copper, Chicken bone ash, corrosion, Inhibitor

1. Introduction

Water pipelines, condensers in ships and power plants, heat conductors, and heat exchangers are just a few of the infrastructure and industrial uses for copper and its alloys. This is a result of their advantageous qualities, which include excellent electrical and thermal conductivity, resistance to corrosion, durability, and wear resistance. Copper has a relatively noble potential, but it is also susceptible to corrosion, particularly in environments with chloride ions [1–4].

The prevention of copper corrosion has attracted a lot of attention over the years, leading to extensive research on various possible inhibitors. Despite the fact that inorganic inhibitors have been studied, new studies have concentrated on organic compounds and their derivatives [5]. Concerns over the high cost of the industrial inorganic and organic inhibitors have led researchers to look into more affordable and eco-friendly corrosion mitigation techniques [6–8]. Utilizing green corrosion inhibitors made from plant and animal byproducts is one such strategy. Particularly, the effectiveness of organic inhibitors extracted from chicken bone ash and other livestock ashes in reducing corrosion on different metal surfaces has been studied [9, 10]. The literature on using these inhibitors on copper surfaces is, however, scarce. The aims of this study are to determine the adsorption parameters in a NaCl solution inhibited with chicken bone ash and to investigate copper's corrosive reactions.

2. Materials and methods

2.1 Material preparation

The copper samples were initially cut into 20 pieces, each measuring 20 by 10 by 2 mm. To achieve a smooth surface, these samples were then treated with grinding and polishing using different grades of emery paper, including 80, 120, 220, 800, 1000, and 1200 μm. The samples were then thoroughly dried, cleaned with ultrasound, and cold stood in epoxy resin. The chicken bone was carefully cleaned with acetone along with warm water to prepare it. After being thoroughly cleaned, the bone was allowed to dry in the sun for 72 hours. The bone was processed into powdered form using a milling machine after being dried and crushed using a rotating crusher. The processed sample was sieved through a 60 μm mesh sieve to create a fine powder. A furnace at a temperature of 200°C was used to calcine a crucible containing 500g of the prepared chicken bone powder for two hours. The final product, chicken bone ash, was finely crushed in a crusher and burr mill to attain the desired particle size after the calcination process. Using an electric sieve apparatus with different sizes ranging from 100 μm to 45 μm, the chicken bone ash was carefully sieved.

*Corresponding author (atibajoshua7@gmail.com)

2.2 Corrosion/Electrochemical analysis

The copper samples were polished using various grades of emery paper, and then they were cleaned with acetone. A three-electrode cell setup was used to clean the samples. The copper sample used as the working electrode had a 1.5 cm^2 exposed surface area. The counter electrode was a graphite rod, and the reference electrode was the silver/silver chloride electrode (Ag/AgCl). In an alkaline environment with 3 wt% NaCl, potentiodynamic polarization techniques were used to examine the corrosion characteristics of the materials, in particular copper, in the presence of the prepared organic inhibitors (chicken bone). An AUTO LAB potentiostat galvanostat (PGSTAT 101), with a temperature range of 30°C to 60°C, was used to conduct the corrosion tests. At each temperature increase, 0.2, 0.4, 0.6, and 0.8 g of inhibitor variations were tested. The anodic and cathodic linear regions could be extrapolated more easily with a scanning rate of 0.001V/sec. Tafel analysis was used to calculate the corrosion potentials, current density, linear polarization resistance, and corrosion rate. Based on the linear polarization resistance (LPR), the inhibition efficiency (%IE) was calculated, and the copper's corrosion resistance was assessed using the potentiodynamic corrosion rate and potentiodynamic polarization corrosion current density. The inhibition efficiency (%IE) can be calculated using the equation 1 given below:

$$\%IE = \frac{i^0_{corr} - i_{corr}}{i^0_{corr}} \times 100, \tag{1}$$

where $i^0{}_{corr}$ and i_{corr} are the absence and presence of corrosion current density of inhibitor, respectively.

2.3 Mathematical Model Optimization

To evaluate how input factors such as inhibitor concentration and operational temperature influence a property parameter, namely corrosion response, we conducted a comprehensive statistical analysis. Design Expert Software 13, with a 95% confidence level, was employed for this purpose. The software allowed us to create mathematical models for each response using second-order regression models, enabling us to make future predictions about the inhibitor's usage. Response Surface Analysis (RSA) encompassed various aspects of the process, including optimizing process parameters, analyzing results, and designing experiments. Utilizing statistical and mathematical techniques, RSA examined the interactions between independent factors and their impact on responses, enabling the development of prediction models from experimental data. To assess the significance and influence of input variables on property responses, we conducted an analysis of variance, as outlined in references [11,12]. The scalar response (R) was determined by employing the experimental design matrix, which detailed the operational parameters at each run level (equation 2).

$$R = a_0 + a_1A + a_2B + a_{12}AB + a_{11}A^2 + a_{22}B^2 + a_{112}A^2B + a_{122}AB^2 + a_{111}A^3 + a_{222}B^3. \tag{2}$$

The variables of temperature and concentration is represented with A and B respectively. a_1, a_2, a_{12}, a_{11}, a_{22}, a_{112}, a_{122}, a_{111}, and a_{222} are coefficients of terminologies.

3. Result and Discussion

3.1 Open Circuit Potential plots of Copper in NaCl/Chickenbone medium

The open circuit potential (OCP) graph of copper in chicken bone inhibited solution of NaCl is shown in Figure 1 at a measured temperature of 30°C. The plot shows that the sample without the inhibitor had the highest potential over the entire 120-second period. This sample had the greatest shift towards the positive region, indicating a higher potential. In contrast, the subsequent inhibitor-treated samples had lower potentials and moved towards the negative potential range. The sample with 0.2g of Chicken bone inhibition had the lowest potential, slightly less than -0.25V. The shift of the curve towards the negative area indicates that the cathodic reaction is more pronounced than the anodic reaction. Moving on, Figure 2 shows a more positive shift in the copper samples' OCP with an increase in Chicken bone inhibition at 60°C.The result leads to the conclusion that as the temperature rises, inhibitions become more potent. There is a clear relationship between the effectiveness of inhibition and temperature, suggesting that higher temperatures contribute to improved inhibition performance [13–16].

3.2 Analysis of Copper's Potentio-dynamic Polarization in a NaCl/Chickenbone Medium

Table 1 shows the electrochemical parameters of copper corrosion in NaCl with different concentrations of chickenbone inhibition, including E_{CORR} (V), J_{CORR} (A/cm^2), corrosion rate (mm/year), and polarization resistance (Ω). The results in the table show that as the concentration of chickenbone inhibition increases, the corrosion rate decreases. This finding is supported further by Figure 3 and 4, which show a decrease in both the cathodic and anodic reactions of copper corrosion.

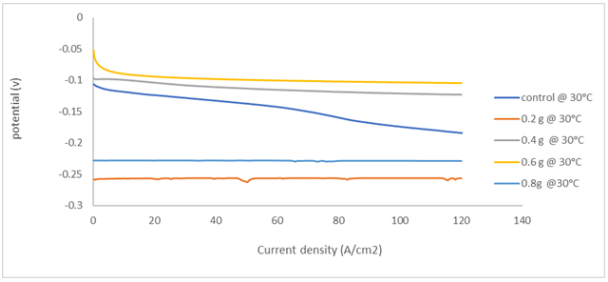

Figure 1: OCP graph for Chicken bone Inhibition @ 30°C

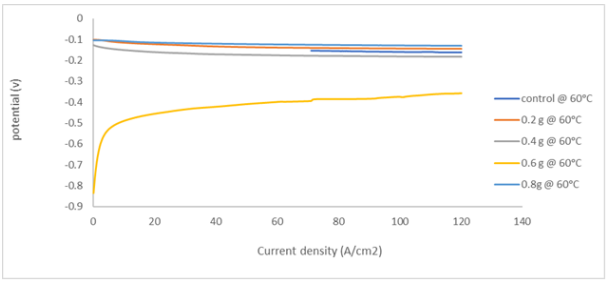

Figure 2: OCP graph for Chicken bone Inhibition @ 60°C

Chicken bone's inhibitive properties are responsible for the corrosion reduction at 30°C and 60°C. Notably, the data in Table 1 and Figures 3 and 4 show a consistent shift of ECORR towards the Negative (Cathodic) region across a wide range of samples and temperature variations. Also, the E_{CORR} deviation across some sample temperatures is less than 0.085V. Based on these findings, it is possible to conclude that the chicken bone inhibitor has cathodic-type inhibition behaviour [17–19].

Temp. of medium (°C)	Conc. of inhibitor (g)	E_{CORR} (V)	J_{CORR} (A/cm^2)	Corrosion rate (mm/year)	Polarization resistance (Ω)
30	Control	-0.304294	1.69E-05	195.963	54.513
	0.2	-0.770591	4.76E-05	55.331	35.722
	0.4	-0.395099	1.14E-04	43.786	21.879
	0.6	0.987073	1.45E-04	23.004	23.247
	0.8	1.311970	3.23E-04	17.988	16.112
40	Control	-1.33383	1.54E-05	179.316	168.858
	0.2	-0.603871	3.48E-04	43.189	48.212
	0.4	-0.919682	4.81E-04	30.977	34.433
	0.6	-1.11331	6.18E-04	25.584	34.225
	0.8	-1.18011	8.73E-04	14.153	24.213
50	Control	-0.936825	1.88E-05	218.959	38.285
	0.2	-0.584499	1.46E-04	47.005	26.056
	0.4	-0.420661	1.77E-04	33.614	22.239
	0.6	-0.350539	1.95E-04	27.563	19.658
	0.8	-1.2227	2.82E-04	21.176	14.286
60	Control	-0.663104	9.66E-05	112.247	69.751
	0.2	-0.457108	1.43E-04	42.567	54.238
	0.4	-0.473323	2.65E-04	30.849	38.146
	0.6	-1.14401	5.16E-04	29.9873	35.047
	0.8	-0.37213	7.54E-04	17.914	16.901

Table 1: Potentiodynamic polarization data for copper in Chickenbone Inhibited NaCl medium

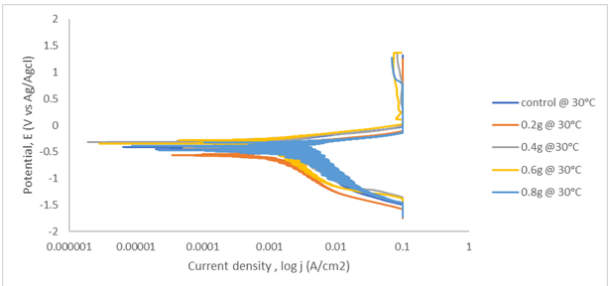

Figure 3: LSV Plot for Chicken bone Inhibition @ 30°C

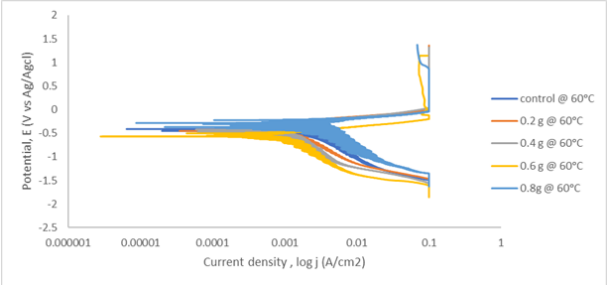

Figure 4: LSV Plot for Chicken bone Inhibition @ 60°C

3.3 Inhibitor Efficiency and Mechanism of Chicken bone

Figure 5 sheds light on the effectiveness of chicken bone's copper inhibition. Notably, the inhibitor performs exceptionally well at 50°C, showing effective inhibition over a range of concentration values. One important finding is that the inhibitor functions as an anodic inhibitor, which adds to its potency. Furthermore, positive improvements in inhibitor performance at lower temperatures are especially encouraging [20]. The absorption of chicken bone ash (CBA) on the copper surface is the process by which it achieves inhibition. By complexing with Cu+ ions during this absorption process, a protective layer is formed that successfully shields the metal surface from any possible attacks by chloride ions. Equation 3 describes this adsorption mechanism [21, 22]:

$$Cu^{+}_{ads} + nCBA \rightarrow [Cu - CBA_n]^{+}_{ads}. \tag{3}$$

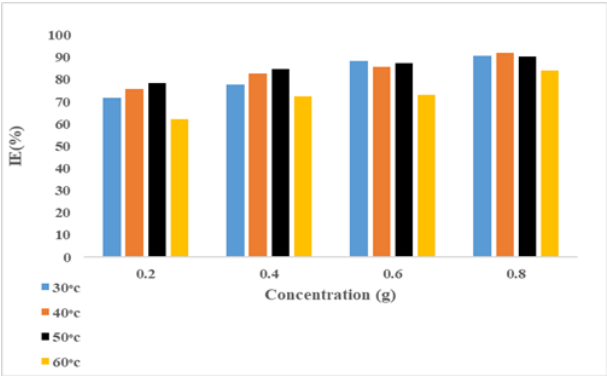

Figure 5: Inhibition efficiency of Chicken bone on copper

3.4 Adsorption Isotherms and Adsorption Parameters

The adhesion of the investigated inhibitor to the metal surface plays a crucial role in the process of corrosion prevention. Various adsorption isotherms, including Temkin, Langmuir, Frumkin, and Freundlich, are commonly used to describe the mechanism of inhibitor adsorption. In this study, the Temkin adsorption isotherm, represented by equation (4), was identified as the most suitable model for fitting the data obtained from electrochemical impedance and potentiodynamic polarization measurements. This finding emphasizes the significance of the Temkin adsorption isotherm in comprehending the behavior of inhibitor adsorption and its impact on corrosion inhibition [23].

$$\theta = BK_{ads} + BlnC_{inh}. \tag{4}$$

The heat of adsorption constant is denoted by the constant B. This isotherm takes into account the interactions between adsorbent and adsorbate. If the minimal and maximum concentration values are ignored, the models determine that the heat of adsorption of all layer molecules decreases linearly rather than logarithmically with coverage, as shown in Figure 6. Table 2 summarizes the K_{ads}(mol-1), Gads (KJmol-1) and R2 values obtained from the Temkin adsorption model. Kads is the force that holds adsorbate and adsorbent together. Larger Kads values indicate greater adsorption and thus better inhibition performance. According to Table 2, the values of K_{ads} decreased with increasing temperature, indicating that the adsorption of Chicken bone ashes on the surface of copper was not favourable, with the exception of 50°C, which had the highest and optimal K_{ads} value, [24–26].

The results show that the negative value of the Gibbs free energy of adsorption, G°_{ads}, confirms the adsorption process's spontaneity and the stability of the adsorbed coating on the copper surface. Furthermore, the adsorbed layer's stability

Temperature (°C)	$K_{ads}(mol^{-1})$	ΔG_{ads} ($KJmol^{-1}$)	R^2	$\ln(K_{ads})$	1/T	$\Delta G_{ads}/T$	B= Slope
30	656.9611	-26.4659	0.9446	6.4876	0.0033	-0.0873	0.1448
40	359.3698	-25.7691	0.9990	5.8844	0.0032	-0.0823	0.1747
50	913.2658	-29.0975	0.9707	6.8170	0.0031	-0.0901	0.1530
60	66.5888	-22.7476	0.9461	4.1985	0.0030	-0.0683	0.2418

Table 2: Adsorption Parameters determined from Temkin isotherm

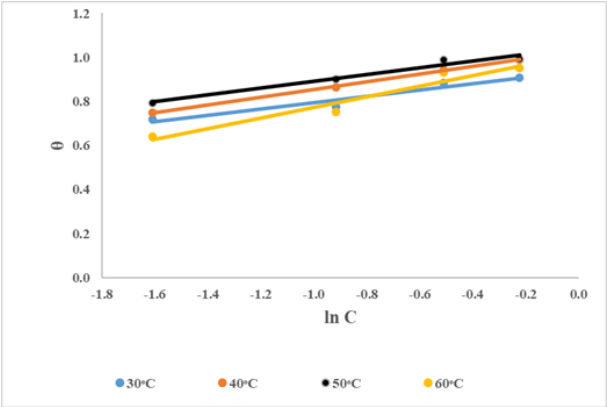

Figure 6: A graph of θ against ln C

improves with increasing temperature, as evidenced by higher absolute values of $G°_{ads}$ at higher temperatures. This implies that higher temperatures favor the adsorption mechanism, possibly due to increased attraction to the adsorbent and increased movement of ions and molecules in the solution. The calculated values of $G°_{ads}$ range from -22.7476 to -29.0975 kJ/mol, indicating that physisorption rather than chemisorption drives the adsorption process. $G°_{ads}$ values below or around -20 kJ/mol are associated with physisorption, while values above -40 kJ/mol are typically associated with chemisorption [27].

3.5 Activation Parameter on the Inhibition Mechanism

The Inhibition mechanism of the corrosion process can easily be understood by temperature variations. The temperature change causes a change in the intensity for all electrochemical system causing changes in the kinetics and the adsorption parameters of a system. The effect oof temperature variation on the corrosion process of copper in a chicken bone inhibited Nacl medium between 30°C to 60°C could be analysed using activation energies. Figure 7 show the relationship between the logarithmic of corrosion density (log J_{CORR}) and temperature reciprocal (1/T), which follows the model of Arrhenius plot for measuring activation energy. Equation 5 and Table 3 shows the formulation for this plot and the values of each parameter respectively.

$$Log\ J_{CORR} = Loglambda - \frac{Ea}{2.30RT}, \tag{5}$$

where, Ea is the activation energy, R molar gas constant and λ the Arrhenius pre-exponential factor.

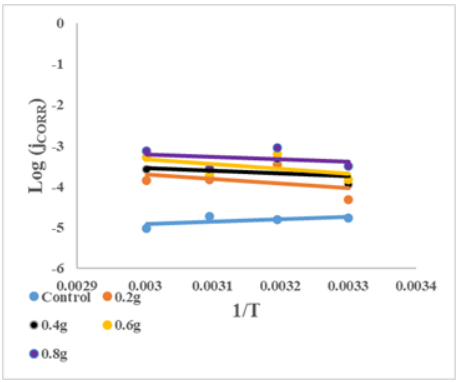

Figure 7: Temperature effect on copper corrosion in NaCl with and without the Chicken bone Inhibition

Figure 7 depicts a linear relationship with a regression coefficient close to unity between the logarithm of corrosion current density obtained from electrochemical measurements and the reciprocal of temperature (1/T). The activation energy (E_a)

and pre-exponential factor (λ) values were calculated from the slope and intercept, respectively, and are shown in Table 3. According to the table, the activation energy decreases with increasing inhibitor concentrations, implying that the chicken bone ash impedes the corrosion process on copper. The observed E_a values are less than the chemisorption threshold of 80 KJ/mol, indicating that the adsorption is physical in nature. This change in E_a causes a decrease in the ash adsorption on copper with increasing temperature, increasing the risk of corrosion in a more aggressive environment [28, 29].

Inhibitor Concentration (g)	Ea (KJ/mol)	λ ($mgcm^{-2}$)	ΔH^o (KJ/mol)	ΔSo (KJ/molK)	ΔG^o (KJ/mol)			
					30°C	40°C	50°C	60°C
Control	12.1009	1.51E-07	-14.7406	-0.3270	84.3282	87.5978	90.8674	94.1370
0.2	21.4673	4.62E-01	18.8276	-0.2028	80.2672	82.2949	84.3226	86.3503
0.4	32.4026	3.60E-02	10.7629	-0.2240	78.6324	80.8723	83.122	85.3522
0.6	41.5348	1.56E+00	19.8951	-0.1926	78.2623	80.1886	82.1149	84.0412
0.8	50.8768	4.44E-02	9.2371	-0.2222	76.5787	78.8012	81.0237	83.2462

Table 3: Activation parameters of Chicken bone inhibitor in NaCl

3.6 Corrosion Rate optimization

A cubic equation model was determined to be the most effective means of encompassing the significance of the interacting factors on copper's corrosion rate response, as depicted in equation 6. The model's robustness and reliability in predicting corrosion rate responses are evident from its high F-value (24.4) and a low P-value (<0.0001). In Table 4, you can find the experimental design detailing the factors influencing copper's corrosion responses within a chicken bone alkaline environment. The optimal combination, as revealed by this study, was a temperature of 40°C and an inhibitor amount of 0.8g, resulting in a corrosion rate of 14.153 mm/yr. Upon a comprehensive analysis of the experimental design, Table 5 was constructed using the central composite design approach. The model's accuracy and its ability to replicate experimental data are underscored by its strong R^2 and low CV% values [11, 30]. The graphical representation in Figure 8 vividly illustrates the impact of these two crucial parameters on chicken bone inhibition of copper. According to the ANOVA results, the best corrosion rate of 8.086 mm/yr was achieved at approximately 34.789°C with an inhibitor amount of 0.789 g of chicken bone ash.

$$R = 29.95 + 26.85A - 11.69B + 14.82AB - 8.09A^2 + 70.20B^2 + 19.51A^2B - 13.95AB^2 - 30.13A^3 - 79.56B^3. \quad (6)$$

Runs	Factor A: Temperature (°C)	Factor B: Concentration (g)	Response 1: Corrosion Rate (mm/yr)
1	40	0.8	14.153
2	60	0.8	17.914
3	30	0.8	17.988
4	50	0.8	21.176
5	30	0.6	23.004
6	40	0.6	25.584
7	50	0.6	27.563
8	60	0.6	29.9873
9	60	0.4	30.849
10	40	0.4	30.977
11	50	0.4	33.614
12	60	0.2	42.567
13	40	0.2	43.189
14	30	0.4	43.786
15	50	0.2	47.005
16	30	0.2	55.331
17	60	0	112.247
18	40	0	179.316
19	30	0	195.963
20	50	0	218.959

Table 4: Experimental design matrix with response to corrosion degradation

Source	SS	DF	MS	F-value	p-value	Remark
Model	72492.74	9	8054.75	24.4	< 0.0001	Sig.
A-Temperature	12568.11	1	568.11	1.72	< 0.0001	Sig.
B-Concentration	128.98	1	128.98	0.3907	< 0.0001	Sig.
AB	1220.26	1	1220.26	3.7	0.0034	Sig.
A^2	258.48	1	258.48	0.783	0.397	Not Sig.
B^2	17246.37	1	17246.37	52.25	< 0.0001	Sig.
A^2B	751.83	1	751.83	2.28	0.1622	Not Sig
AB^2	378.42	1	378.42	1.15	0.3095	Not Sig.
A^3	717.18	1	717.18	2.17	0.1713	Not Sig.
B^3	5554.19	1	5554.19	16.83	0.0021	Sig.
Residual	3300.97	10	330.1			
Cor Total	75793.71	19				

Table 5: Variance analysis (ANOVA) in response to corrosion on copper [$\mathbf{R}^2 = 95.64\%$; Adjusted $\mathbf{R}^2 = 91.73\%$; predicted $\mathbf{R}^2 = 73.22\%$; CV%= 11.31. ** SS- Sum of square; DF- Degree of Freedom; MS- Mean square; Sig.- Significant**]

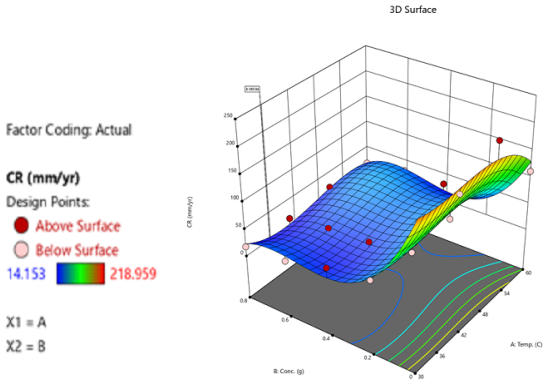

Figure 8: optimization Parameter plots of Chicken bone ash on copper

4. Conclusion

Numerous significant findings have emerged from our experimental analysis. Firstly, the result of the polarization experiments strongly suggest that chicken bone ash acts primarily as a cathodic inhibitor. Furthermore, it can be inferred that the metal surface displays a favourable response to the adsorption of the inhibitor, as indicated by trends in the Temkin Adsorption parameter (K_{ads}). Our Gibbs free energy calculations also point to the predominantly physisorption-based adsorption of chicken bone ash on the copper surface. Notably, we discovered that the optimal temperature for achieving efficient inhibition with chicken bone ash is 50°C. Additionally, through statistical optimization, we determined that the most effective conditions, with temperatures around 34.789°C and an inhibitor concentration of 0.789 g, resulted in an optimized corrosion rate of 8.086 mm/yr.

Ethical Approval

Not applicable to this paper.

Competing interests

The authors declare no competing interests.

Authors' contributions

Ojo S. I. Fayomi: Research conceptualization and supervision. Joshua O. Atiba: Writing of manuscript and tables and experimentation.

Funding

The authors have no relevant financial or non-financial interest to disclose.

References

[1] Al Kharafi, F. M., Al-Awadi, N. A., Ghayad, I. M., Abdullah, R. M., & Ibrahim, M. R. (2011). Corrosion protection of copper using azoles applied on its surface at high temperature under vacuum. *International Journal of Electrochemical Science, 6*(5), 1562–1571.

[2] Antonijevic, M. M., Alagic, S. C., Petrovic, M. B., Radovanovic, M. B., & Stamenkovic, A. T. (2009). The influence of pH on electrochemical behavior of copper in presence of chloride ions. *International Journal of Electrochemical Science, 4*(4), 516–524.

[3] Sherif, E.-S. M., & Ahmed, A. H. (2010). Synthesizing new hydrazone derivatives and studying their effects on the inhibition of copper corrosion in sodium chloride solutions. *Synthesis and Reactivity in Inorganic, Metal-Organic, and Nano-Metal Chemistry, 40*(6), 365–372.

[4] Sherif, E. S. M. (2012). Electrochemical and gravimetric study on the corrosion and corrosion inhibition of pure copper in sodium chloride solutions by two azole derivatives. *International Journal of Electrochemical Science, 7*(2), 1482–1495.

[5] Mihajlović, M. B. P., & Antonijević, M. M. (2015). Copper corrosion inhibitors. Period 2008-2014. A review. *International Journal of Electrochemical Science, 10*(2), 1027–1053.

[6] Haldhar, R., Prasad, D., & Saxena, A. (2018). Armoracia rusticana as sustainable and eco-friendly corrosion inhibitor for mild steel in 0.5 M sulphuric acid: Experimental and theoretical investigations. *Journal of Environmental Chemical Engineering, 6*(4), 5230–5238.

[7] Rosli, N. R., Yusuf, S. M., Sauki, A., & Razali, W. M. R. W. (2019). Musa sapientum (Banana) peels as green corrosion inhibitor for mild steel. *Key Engineering Materials, 797*, 230–239.

[8] Sun, X., Qiang, Y., Hou, B., Zhu, H., & Tian, H. (2022). Cabbage extract as an eco-friendly corrosion inhibitor for X70 steel in hydrochloric acid medium. *Journal of Molecular Liquids, 362*, 119733.

[9] Loto, Roland T, & Busari, A. A. (2022). Inhibition effect of cow bone soot on low carbon steel corrosion in artificial concrete pore environment. *Journal of Physics: Conference Series, 2256*(1), 12024.

[10] Loto, Roland Tolulope, & Busari, A. (2019). Electrochemical study of the inhibition effect of cow bone ash on the corrosion resistance of mild steel in artificial concrete pore solution. *Cogent Engineering, 6*(1), 1644710.

[11] Goh, K.-H., Lim, T.-T., & Chui, P.-C. (2008). Evaluation of the effect of dosage, pH and contact time on high-dose phosphate inhibition for copper corrosion control using response surface methodology (RSM). *Corrosion Science, 50*(4), 918–927.

[12] Zhang, R., Cao, S., & Pan, H. (2018). Evaluation of hollow copper strands corrosion behavior in stator cooling water using response surface methodology. *Materials and Corrosion, 69*(6), 804–813.

[13] Berdimurodov, E., Kholikov, A., Akbarov, K., Obot, I. B., & Guo, L. (2021). Thioglycoluril derivative as a new and effective corrosion inhibitor for low carbon steel in a 1 M HCl medium: Experimental and theoretical investigation. *Journal of Molecular Structure, 1234*, 130165.

[14] Murulana, L. C., Kabanda, M. M., & Ebenso, E. E. (2015). Experimental and theoretical studies on the corrosion inhibition of mild steel by some sulphonamides in aqueous HCl. *RSC Advances, 5*(36), 28743–28761.

[15] Paszenda, Z., Walke, W., & Jadacka, S. (2010). Electrochemical investigations of Ti6Al4V and Ti6Al7Nb alloys used on implants in bone surgery. *Journal of Achievements in Materials and Manufacturing Engineering, 38*(1), 24–32.

[16] Sherif, E.-S. M. (2011). Effects of 5-(3-aminophenyl)-tetrazole on the inhibition of unalloyed iron corrosion in aerated 3.5% sodium chloride solutions as a corrosion inhibitor. *Materials Chemistry and Physics, 129*(3), 961–967.

[17] Amin, M. A., Abd El-Rehim, S. S., El-Sherbini, E. E. F., & Bayoumi, R. S. (2007). The inhibition of low carbon steel corrosion in hydrochloric acid solutions by succinic acid: Part I. Weight loss, polarization, EIS, PZC, EDX and SEM studies. *Electrochimica Acta, 52*(11), 3588–3600.

[18] Amin, M. A., Khaled, K. F., & Fadl-Allah, S. A. (2010). Testing validity of the Tafel extrapolation method for monitoring corrosion of cold rolled steel in HCl solutions–experimental and theoretical studies. *Corrosion Science, 52*(1), 140–151.

[19] Sherif, E. M., & Park, S.-M. (2006). 2-Amino-5-ethyl-1, 3, 4-thiadiazole as a corrosion inhibitor for copper in 3.0% NaCl solutions. *Corrosion Science, 48*(12), 4065–4079.

[20] Oguzie, E. E., Li, Y., & Wang, F. H. (2007). Effect of 2-amino-3-mercaptopropanoic acid (cysteine) on the corrosion behaviour of low carbon steel in sulphuric acid. *Electrochimica Acta, 53*(2), 909–914.

[21] Gao, L., Peng, S., Huang, X., & Gong, Z. (2020). Applied Surface Science A combined experimental and theoretical study of papain as a biological eco-friendly inhibitor for copper corrosion in H 2 SO 4 medium. *Applied Surface Science, 511*(December 2019), 145446.

[22] Tasić, Ž. Z., Petrović Mihajlović, M. B., Radovanović, M. B., & Antonijević, M. M. (2018). Electrochemical investigations of copper corrosion inhibition by azithromycin in 0.9% NaCl. *Journal of Molecular Liquids, 265,* 687–692.

[23] Elendu, I. O., Odulanmi, O. A., Fayomi, O. S. I., Williams, A. B., & Daramola, M. (2021). Passivation behaviour and localized corrosion activities of non-toxic surfactant derivatives on Copper. IOP Conference Series: *Materials Science and Engineering, 1107*(1), 012224.

[24] Dada, A O, Olalekan, A. P., Olatunya, A. M., & Dada, O. (2012). Langmuir, Freundlich, Temkin and Dubinin–Radushkevich isotherms studies of equilibrium sorption of Zn2+ unto phosphoric acid modified rice husk. *IOSR Journal of Applied Chemistry, 3*(1), 38–45.

[25] Dada, Adewumi O, Ojediran, J. O., & Olalekan, A. P. (2013). Sorption of Pb2+ from aqueous solution unto modified rice husk: isotherms studies. *Advances in Physical Chemistry, 2013*, 1–6.

[26] Fateh, A., Aliofkhazraei, M., & Rezvanian, A. R. (2020). Review of corrosive environments for copper and its corrosion inhibitors. *Arabian Journal of Chemistry, 13*(1), 481–544.

[27] Ahamad, I., Prasad, R., & Quraishi, M. A. (2010). Adsorption and inhibitive properties of some new Mannich bases of Isatin derivatives on corrosion of mild steel in acidic media. *Corrosion Science, 52*(4), 1472–1481.

[28] Hippolyte, C. N., Serge, B. Y., Sagne, A., Creus, J., & Albert, T. (2018). Nicotinamide inhibition properties for copper corrosion in 3.5% NaCl solution: experimental and theorical investigations. *Journal of Materials Science and Chemical Engineering, 6*(03), 100.

[29] Oguzie, E. E., Onuoha, G. N., & Onuchukwu, A. I. (2005). Inhibitory mechanism of mild steel corrosion in 2 M sulphuric acid solution by methylene blue dye. *Materials Chemistry and Physics, 89*(2–3), 305–311.

[30] Omoegun, O. G., Fayomi, O. S. I., & Atiba, J. O. (2023). Investigation of the Corrosive Behavior and Adsorption Parameters of Copper in a Cowbone Ash Inhibited Alkaline Environment. *Journal of Bio- and Tribo-Corrosion, 9*(4). https://doi.org/10.1007/s40735-023-00794-1